Vitamin C deficiency induces hypoglycemia and cognitive disorder through S-nitrosylation-mediated activation of glycogen synthase kinase 3β

Yingying Shu [a,b,1], Chaochun Zou [a,b,**,1], Yuqing Cai [a,b], Qiangqiang He [c], Xiaowei Wu [d], Haibin Zhu [d], Meiyu Qv [c], Yunqi Chao [a,b], Chengyun Xu [b,c], Lanfang Tang [b], Ximei Wu [c,*]

[a] Department of Endocrinology, The Children's Hospital of Zhejiang University School of Medicine, Hangzhou, 310053, China
[b] National Clinical Research Center for Child Health, The Children's Hospital of Zhejiang University School of Medicine, Hangzhou, 310053, China
[c] Department of Pharmacology, Zhejiang University School of Medicine, Hangzhou, 310058, China
[d] Department of Obstetrics and Gynecology, The First Affiliated Hospital, Zhejiang University School of Medicine, Hangzhou, 310003, China

ARTICLE INFO

ABSTRACT

Vitamin C (VC, L-ascorbic acid) is an essential nutrient that plays a key role in metabolism and functions as a potent antioxidant in regulating the S-nitrosylation and denitrosylation of target proteins. The precise function of VC deprivation in glucose homeostasis is still unknown. In the absence of L-gulono-1,4-lactone oxidoreductase, an essential enzyme for the last step of VC synthesis, VC deprivation resulted in persistent hypoglycemia and subsequent impairment of cognitive functions in female but not male mouse pups. The cognitive disorders caused by VC deprivation were largely reversed when these female pups were given glucose. VC deprivation-induced S-nitrosylation of glycogen synthase kinase 3β (GSK3β) at Cys14, which activated GSK3β and inactivated glycogen synthase to decrease glycogen synthesis and storage under the feeding condition, while VC deprivation inactivated glycogen phosphorylase to decrease glycogenolysis under the fasting condition, ultimately leading to hypoglycemia and cognitive disorders. Treatment with Nω-Nitro-L-arginine methyl ester (L-NAME), a specific inhibitor of nitric oxide synthase, on the other hand, effectively prevented S-nitrosylation and activation of GSK3β in female pups in response to the VC deprivation and reversed hypoglycemia and cognitive disorders. Overall, this research identifies S-nitrosylation of GSK3β and subsequent GSK3β activation as a previously unknown mechanism controlling glucose homeostasis in female pups in response to VC deprivation, implying that VC supplementation in the prevention of hypoglycemia and cognitive disorders should be considered in the certain groups of people, particularly young females.

1. Introduction

Glucose homeostasis in circulation is dynamically regulated by both the glucose production from liver and kidney and glucose usage by peripheral tissues. In the fasted status, glucose is produced by gluconeogenesis and glycogenolysis, whereas glucose is stored by promoting glycogen synthesis and suppressing hepatic glucose output in the postprandial status [1]. Hepatic gluconeogenesis is predominantly determined by glucose-6-phosphatase (G6PC) and phosphoenolpyruvate carboxykinase (PEPCK) encoded by two genes *Pck1* (cytosolic form) and

Pck2 (mitochondrial form) [2], whereas hepatic glycogenolysis is rate-limited by glycogen phosphorylase (GP). In contrast, glycogen synthesis is an opposite process to glycogenolysis and rate-limited by glycogen synthase (GS), which is inactivated and activated by phosphorylation and dephosphorylation at Ser641, respectively [3].

Hyperglycemia and hypoglycemia are two medical conditions occurring due primarily to the disorder of glycometabolism. Long-lasting hyperglycemia causes diabetes and its complications. Hypoglycemia, an often under-appreciated problem, is usually associated with diabetic glucose-lowering therapy, but other drugs and a variety of

conditions also can cause hypoglycemia in people without diabetes [4, 5]. Hypoglycemia is related to a variety of symptoms progressing from sweating to seizures and depending on its severity and duration. Untreated hypoglycemia can lead to a series of severe neurological consequences, and impaired cognitive function has potentially deleterious and cumulative long-term effects on intellectual function, especially in young children [6,7].

Protein S-nitrosylation or denitrosylation is a dynamic and reversible post-translational modification by coupling or uncoupling of nitric oxide (NO) with the reactive thiol group of a protein cysteine residue to form or decompose an S-nitrosothiol (SNO), respectively [8,9]. S-nitrosylation or denitrosylation on a cysteine residue of proteins depends on the redox state of cell loci. Vitamin C (VC, L-ascorbic acid), an essential anti-oxidant, not only functions as a scavenger of oxidizing free radicals and prevents the oxidation of other reductants [10,11], but also participates in the denitrosylation of proteins, representing a general mechanism for turning off NO-mediated signaling transduction that is initiated by protein S-nitrosylation [12,13].

Except for its role in protein S-denitrosylation, VC participates in the diabetes-associated glucose metabolism. VC supplement ameliorates symptoms of type 2 diabetes in obese mice with hyperglycemia and diabetic glomerular injury in rats [14], and prevents dexamethasone-induced glucose intolerance as well as tumor necrosis factor-α (TNF-α)-induced insulin resistance [15]. In addition, VC inhibits glucose uptake and lactate production in primary rat adipocytes [16], and especially prevents islet against autoimmunity to lower the risk of type 1 diabetes in children [17]. However, the specific role of VC deprivation in the regulation of glycometabolism remains unknown.

Though persistent deprivation of VC leads to scurvy in a certain condition, there are certain groups of people encountering the risk of VC deficiency, including people who are addicted to drugs or alcohol, people who live on a low income, people with medical conditions such as Crohn's disease or ulcerative colitis, pediatric patients with advanced chronic kidney disease, children with severely restricted diets attributable to psychiatric or developmental problems, older people who eat a less varied diet and smokers [18–22]. For instance, a 17-year-old male who suffers from hereditary fructose intolerance exhibits severe VC deficiency (serum VC < 10 μM; normal range: 26–84 μM), hepatomegaly, proximal tubular dysfunction, and hypoglycemia as well [23].

In the present study, we attempted to assess the role of VC deprivation in glucose metabolism in mice absent of *L-gulono-1,4-lactone oxidoreductase* (*Gulo$^{-/-}$*), which catalyzes the last step of VC biosynthesis. We found that VC deprivation induced the S-nitrosylation of glycogen synthase kinase 3β (GSK3β) at Cys14, which activated GSK3β and in turn inactivated GS to decrease the glycogen synthesis and storage under fed conditions, and meanwhile VC deprivation inactivated GP to decrease the glycogenolysis under fasting conditions, eventually leading to the hypoglycemia and consequent cognitive disorders.

2. Research design and methods

2.1. Animal care and handling

Gulo$^{-/-}$ mice on the C57BL/6 genetic background was generated by transcription activator-like effector nuclease (TALEN) technique as described previously [24]. *Gulo$^{-/-}$* mice could not synthesize VC by themselves (serum VC: ~10 μM) and were maintained with tap water containing 3.3 g/L of VC (serum VC: ~60 μM) [14]. All mice were housed in a specific pathogen free animal facility of Zhejiang University and allowed free access to regular rodent chow or VC-free rodent chow (Trophic Animal Feed High-tech Corporation, Nantong, China). All animal cares and handling procedures (Protocol No. 20180226-003) were approved by the Institutional Animal Care and Use Committee of Zhejiang University.

2.2. Experimental designs

Female and male *Gulo$^{-/-}$* mice were maintained with tap water containing 3.3 g/L of VC, and crossed to generate *Gulo$^{-/-}$* pups. Pups were all weaned at day 21 after birth and 22-day-old *Gulo$^{-/-}$* pups were then randomly and evenly divided into four groups: (1) male or female pups supplemented with 3.3 g/L of VC (VC+), (2) male or female pups deprived of VC (VC-). Alternatively, 22-day-old female *Gulo$^{-/-}$* pups supplemented with or without 3.3 g/L of VC, were peritoneally injected with or without L-NAME at 0.8 mg/10 body weight, once daily, for five consecutive weeks. All pups were allowed free access to VC-free rodent chow. After fasted for 16 h, blood glucose was measured by a glucometer (Onetouch Ultra, Johnson, LifeScan Europe, UK). Meanwhile, blood samples were harvested and centrifuged at 3000 g for 20 min. Serum was stored at −80 °C until analysis. In addition, after livers were removed and weighed, the left lateral lobes were fixed with 4% formaldehyde and the remaining lobes were all frozen in liquid nitrogen and then stored at −80 °C.

2.3. Pyruvate tolerance test and intraperitoneal glucose tolerance test

Pyruvate tolerance test (PTT) and intraperitoneal glucose tolerance test (IPGTT) were performed in female pups after VC deprivation for 3 (6-week-old) and 5 weeks (8-week-old), respectively. Pups were fasted for 16 h, and then intraperitoneally (i.p.) injected with sodium pyruvate (Sigma) at 1.5 g/kg body weight for PTT or with D-glucose (Sigma) at 1 g/kg body weight for IPGTT, as previously described [25]. Blood glucose was measured at 0, 15, 30, 60, 90, and 120 min after the injection.

2.4. Biochemical and histological analyses

Blood samples were used to determine the levels of insulin or glucagon using a mouse insulin or glucagon enzyme-linked immunosorbent assays (ELISA) kit (Nanjing Jiancheng Bioengineering Institute, Nanjing, China) according to the manufacturer's instructions, respectively. The Periodic Acid-Schiff (PAS) and immunohistochemistry staining were performed as previously described [14,26]. The primary antibodies against p-Ser641-GS (1:200 dilution, ET1602-13; HuaAn Biotechnology, Hangzhou, China), p-Ser15-glycogen phosphorylase L (PYGL; 1:200 dilution, ab227043; Abcam, Cambridge, UK), and p-Ser9-GSK3β (1:50 dilution, ab131097; Abcam) were used in the experiments.

2.5. Isolation and culture of mouse primary hepatocytes

Primary mouse hepatocytes were isolated from female *Gulo$^{-/-}$* pups with deprivation of VC for 3-week by digesting the livers with type II collagenase (CAT LS004176; Worthington, Lakewood, CO) as described previously [27]. Isolated hepatocytes were seeded into 6-well-plate covered with type I collagen (CAT 354236; Corning, Glendale, AZ) and successfully attached at 2 h post-inoculation. VC was added to stimulate primary mouse hepatocytes for the indicated times, and then cells were harvested for western blotting analyses.

2.6. Cell cultures and transfection

Human hepatocytes L02 cells were gifted from Prof. Zhi Chen at the First Affiliated Hospital, Zhejiang University School of Medicine, and maintained in Dulbecco's Modified Eagle Medium (DMEM) supplemented with 10% fetal bovine serum (Life Technologies, Carlsbad, CA) and 1% penicillin-streptomycin (Sigma). Human hepatocarcinoma HepG2 cells from Chinese Academy of Sciences (Shanghai, China) were cultured in Modified Eagle Medium (MEM) containing 10% FBS, 1% L-glutamine (Invitrogen, Grand Island, NY), 1% non-essential Amino Acids (Invitrogen), and 1% sodium pyruvate (Invitrogen). VC (Sigma), N6022 (S7589; Selleckchem, Huston, TX), and Nω-Nitro-L-arginine

methyl ester (L-NAME, S2877; Selleckchem) were used to stimulate L02 and HepG2 cells. Cell lines were all incubated at 37 °C with 5% CO_2. pCMV-3 × Flag-GSK3β construct was obtained from MiaoLingBio (Wuhan, China) and verified by DNA sequencing. Cys14Ser (C14S) mutation of GSK3β was introduced by using a KOD-Plus-Mutagenesis Kit (SMK-101; Toyobo, Osaka, Japan) according to the manufacturer's instruction. Transient transfection was performed by using Hieff Trans™ Liposomal Transfection Reagent (40802ES03; Yeasen Biotechnology, Shanghai, China) as previously described [28].

2.7. In vitro S-Nitrosylation assay

In vitro S-nitrosylation assays were performed using a Pierce™ S-nitrosylation Western Blot Kit (90105; Thermo scientific, Waltham, MA) with modification. All reactions were performed in the dark place to avoid light exposure after immunoprecipitation and enrichment of GSK3β. Protein lysates at 1 mg/mL were prepared in 100 μl HENS buffer (Sigma) and S-nitrosylated cysteines were labelled with a non-biological iodoTMT™ Reagent as described previously [29].

2.8. Western blotting

Proteins from livers, primary hepatocytes, and cell lines were extracted by cell lysis buffer (Beyotime Biotechnology, Shanghai, China) containing protease inhibitor and phosphatase inhibitors (Bimake, Houston, TX). 50 μg protein was separated by 8–12% SDS-PAGE, transferred onto a nitrocellulose membrane, and incubated with primary antibodies at 4 °C overnight. The following primary antibodies were used in the experiments: anti-Pck1 (1:1000 dilution, ab70358), anti-p-Forkhead box O1a (Foxo1a; 1:1000 dilution, ab131339), anti-p-PYGL (1:1000 dilution, ab227043), and anti-p-GSK3β (1:1000 dilution, ab131097) were purchased from Abcam, anti-PYGL (1:1000 dilution, NBP1-86182) was purchased from Novus Biologicals (Centennial, CO), anti-Flag (1:2000 dilution, TA180144) was purchased from Origene (Rockville, MD), anti-Pck2 (1:1000 dilution, ET7107-29), anti-Foxo1a (1:1000 dilution, ET1608-25), anti-p-GS (1:1000 dilution, ET1602-13), anti-GS2 (1:1000 dilution, ER1909-76), anti-GSK3β (1:1000 dilution, ET1607-71), anti-Gapdh (1:5000 dilution, R1210-1) and anti-α-tubulin (1:2000 dilution, ER130905) were purchased from HuaAn Biotechnology. IRDye 680 (926–68070; LI-COR, Lincoln, NE) or 800s antibody (926–32211, LI-COR) was used as the second antibodies. Immunoreactive bands were visualized by Odyssey Infrared Imaging System (LI-COR) and semi-quantified by ImageJ (NIH, Bethesda, MD). The phosphorylated protein was normalized to its total protein, whereas total protein was normalized to either Gapdh or α-tubulin. The first band was defined as 1.

2.9. Morris water maze

Female $Gulo^{-/-}$ pups at 3 weeks old randomly received tap water containing 3.3 g/L of VC, 2 g/L of glucose, or neither VC nor glucose for three consecutive weeks. Alternatively, female $Gulo^{-/-}$ pups supplemented with or without 3.3 g/L of VC, were peritoneally injected with or without L-NAME at 0.8 mg/10 body weight, once daily, for four consecutive weeks. These groups of pups were then subjected to the tests for learning and memory abilities by using a Morris water maze as described previously [30].

2.10. Statistical analysis

Numeral data from animal and cell experiments were expressed as Mean ± SEM or Mean ± SD. Statistical analyses were conducted by one-way ANOVA and Dunnett's multiple comparison tests or by Welch's t-test (Graphpad Software Inc., La Jolla, CA). Statistical significance was assessed at $p < 0.05$ and $p < 0.01$. All experiments were repeated independently three times with similar results, and the representative data were shown.

3. Results

3.1. VC deprivation lowered the fasting serum glucose in a sex-specific manner

In $Gulo^{-/-}$ mice, VC deprivation for 2 weeks reduced serum VC by 85%, while a 3.3 g/L VC supplement in drinking water maintained the normal serum VC level (approximately 60 μM) [14,15]. To determine the role of VC deprivation in regulating fasting serum glucose (FSG), female and male $Gulo^{-/-}$ pups were started on VC deprivation at 3 weeks old, and FSG levels were measured once a week for 5 weeks. We chose 5 weeks as the observational period because, after 5 weeks of VC deprivation, some $Gulo^{-/-}$ pups died. FSG levels in female $Gulo^{-/-}$ pups dropped significantly at week 3 after VC deprivation and remained low until week 5 after VC deprivation (Fig. 1A). FSG levels in male $Gulo^{-/-}$ pups, on the other hand, dropped significantly at week 5 after VC deprivation (Fig. 1B). When VC-deprived female $Gulo^{-/-}$ pups were compared to VC-supplemented female $Gulo^{-/-}$ pups, the area under the curve (AUC) of FSG values from weeks 3–5 was significantly reduced by 24%. (Fig. 1C). Although the AUC of FSG values decreased by 11% from week 3–5 in VC-deprived male $Gulo^{-/-}$ pups compared to VC-supplemented male $Gulo^{-/-}$ pups, there was no statistical difference in this decrease (Fig. 1D). Thus, VC deprivation reduced FSG in female $Gulo^{-/-}$ pups but not in male $Gulo^{-/-}$ pups.

We measured the average food intake of 24 h relative to body weight in female and male $Gulo^{-/-}$ pups after 3 weeks of VC deprivation to rule out the possibility that insufficient food intake caused hypoglycemia. Female and male $Gulo^{-/-}$ pups with VC deficiency had significantly lower average food intakes in equal measure over 24 h (Fig. 1E and F). Similarly, from weeks 3–5 after VC deprivation, the body weights of VC-deprived female and male $Gulo^{-/-}$ pups were significantly reduced to the same extent (Figs. S1A and B). Also, when both female and male $Gulo^{-/-}$ pups were denied VC for 3 weeks, their average 24-h water intake was reduced indiscriminately concerning body weight. (Figs. S1C and D).

We compared FSG levels and body weights in wild-type pups and $Gulo^{-/-}$ pups supplemented with 3.3 g/L VC to rule out the possibility that hypoglycemia in female $Gulo^{-/-}$ pups was caused by genetic manipulation or knockout of the $Gulo$ gene. Compared to female wild-type pups, genetic manipulation or knockout of the $Gulo$ gene did not affect FSG levels or body weights in female $Gulo^{-/-}$ pups supplemented with 3.3 g/L VC (Figs. S2A and B). Also, measurements of fasting serum insulin and glucagon levels in female $Gulo^{-/-}$ pups consistently showed that VC deprivation for 4 weeks did not affect serum insulin or glucagon levels (Figs. S3A and B). Finally, measurements of the liver coefficient revealed that 5 weeks of VC deprivation significantly reduced the liver coefficient in both female and male $Gulo^{-/-}$ pups, though the decrease was more pronounced in males than females (Figs. S4A and B). In $Gulo^{-/-}$ pups, VC deprivation reduced FSG in a sex-dependent manner, but not in a food intake-, genetic manipulation-, or hormone-dependent manner.

3.2. VC deprivation affected the glycometabolism in female Gulo$^{-/-}$ pups

We used Tandem Mass Tag (TMT)-based quantitative proteomics analyses in the livers of female $Gulo^{-/-}$ pups after 3 weeks of VC deprivation to investigate the potential mechanism underlying VC deprivation-induced hypoglycemia. There were 5651 proteins found with a normal distribution (Supplementary Table 1). Differentially expressed proteins (DEPs) were defined as proteins with a fold change of >1.2 or <0.833 (p < 0.05). 406 DEPs were found among the 5651 proteins, with 156 and 250 of them significantly up-regulated and down-regulated, respectively (Supplementary Table 2). The volcano plot displayed the statistical results of protein quantification. (Fig. 2A). Similarly, pathway enrichment analysis using the Kyoto Encyclopedia of
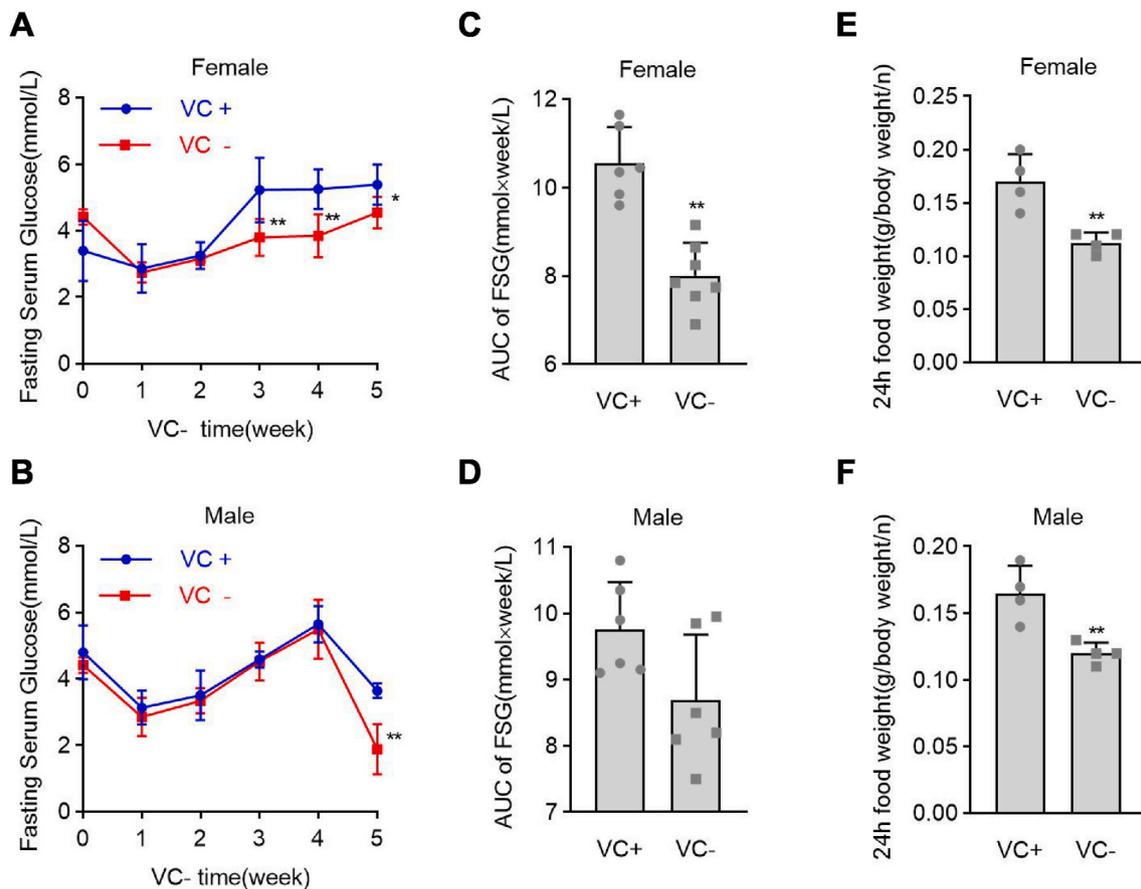
Fig. 1. Female $Gulo^{-/-}$ pups had lower fasting serum glucose levels after VC deprivation. Male or female pups at 22 days old were subjected to VC supplementation (VC+) or deprivation (VC-) for 5 weeks. Before blood isolation and serum glucose measurement, each group of pups was starved for 16 h. (**A and B**) Fasting serum glucose (FSG) levels in male and female pups after VC deprivation for the indicated times. (**C and D**) FSG values for the area under the curve (AUC) were calculated during a 3 to 5-week period of VC deprivation. (**E and F**) The average food intake of 24 h per pup relative to body weight was calculated during the 3 weeks of VC deprivation. Welch's *t*-test, n = 6, mean SD; *$p < 0.05$, **$p < 0.01$ versus VC+.

Genes and Genomes (KEGG) was used to determine the functions of DEPs. DEPs were found in 276 KEGG pathways in VC-deficient pups (Supplementary Table 3). We focused on the metabolic and glucagon signaling pathways among the top 20 significant pathways (Fig. 2B) to investigate the mechanism underlying VC deprivation-induced hypoglycemia. Hierarchical clustering analysis of DEPs indicated that the glucagon signaling pathway was composed of 7 DEPs (Fig. 2C), including Acetyl-CoA carboxylase 1 (Acaca), Acetyl-CoA carboxylase 2 (Acacb), Phosphoglycerate mutase 2 (Pgam2), Solute carrier family 2 facilitated glucose transporter member 2 (Slc2a2), GP of muscle form (fold change = 0.4338), GP of brain form (fold change = 0.8146), and GP of the liver form (fold change = 0.8328). In female $Gulo^{-/-}$ pups, VC deprivation affected the glucose metabolism signaling pathway.

3.3. VC deprivation affected glycogen synthesis and glycogenolysis but not gluconeogenesis and peripheral glucose uptake

We used western blotting and immunohistochemistry staining in the livers of female $Gulo^{-/-}$ pups who had VC deprivation to investigate the role of VC deprivation in glycometabolism. We investigated the flux of gluconeogenesis because it is an important source of glucose supplementation during fasting. VC deprivation for 3, 4, or 5 weeks did not affect the protein levels of rate-limiting enzymes of gluconeogenesis such as Pck1 and Pck2, as well as their upstream transcription factor FoxO1a (Figs. S5A–H). The capacity of hepatic gluconeogenesis was then assessed using PTT assays, which revealed that female $Gulo^{-/-}$ pups who had been deprived of VC for 5 weeks had no significant blood

glucose changes following a pyruvate challenge in the fasting condition (Figs. S5I and J). Female $Gulo^{-/-}$ pups with VC deprivation for 3 weeks were analyzed for their glucose-disposal capacity using an IPGTT to see what effect VC deprivation had on peripheral tissue glucose uptake. Female $Gulo^{-/-}$ pups with 3 weeks of VC deprivation had no significant blood glucose changes after a glucose challenge under fasting conditions, according to the findings (Fig. S5K and L). Gluconeogenesis and peripheral glucose uptake were both unaffected by VC deprivation.

To investigate the role of VC deprivation in glycogenesis and glycogenolysis, we performed western blotting and immunohistochemistry analyses in livers for GS, a rate-limiting enzyme for glycogen synthesis that is inactivated by phosphorylation at Ser641 [1], and GP that is a rate-limiting enzyme involved in breaking the α-1, 4-glycosidic linkages from the terminal end of a glycogen chain and activated by phosphorylation at Ser15 [1,31]. Compared to VC supplementation for 3, 4, or 5 weeks, western blotting analyses revealed that VC deprivation for 3, 4, or 5 weeks robustly induced p-Ser641-GS levels in female $Gulo^{-/-}$ pups under the fed condition (Fig. 3A, E, I). Immunohisto-chemistry analysis confirmed this observation, showing that p-Ser641-GS staining was diffusely distributed in liver sections, especially around the central vein, and was more robustly detected in the livers of female $Gulo^{-/-}$ pups with VC deprivation than with VC supplementation (Fig. 3C, G, K). Western blotting analyses confirmed the proteomic findings, showing that VC deprivation for 3, 4, or 5 weeks reduced the p-Ser15-PYGL levels of livers in female $Gulo^{-/-}$ pups when compared to VC supplementation for 3, 4, or 5 weeks, respectively (Fig. 3B, F, J). Similarly, immunohistochemistry analyses revealed that
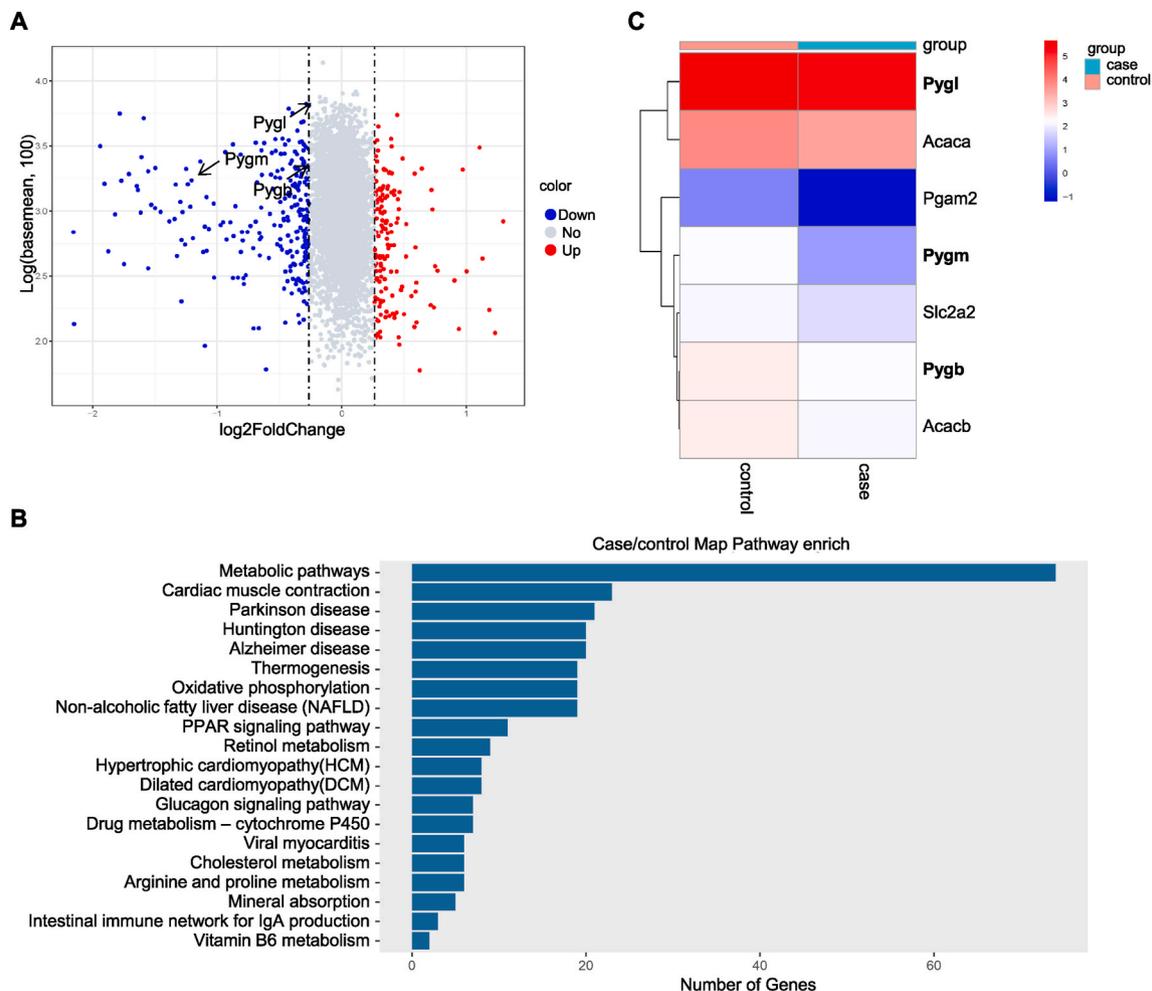
Fig. 2. In female $Gulo^{-/-}$ pups, GP was significantly down-regulated after VC deprivation. TMT-based comparative proteomics analyses for female pups' livers supplemented or depleted of VC for 3 weeks. (**A**) A volcano plot of DEPs in liver tissues. All proteins were plotted on the x-axis with log2 fold change and log10 (the sum of intensity in two samples) on the y-axis. The red dots in the upper right (ratio>1.2) and blue dots in the upper left (ratio<0.833) sections with $p < 0.05$ represent proteins that were significantly up-or down-regulated between groups. Gray dots represented proteins that were identical in the two compared groups. (**B**) KEGG pathway enrichment analysis of the top twenty enrichment scores for DEPs. The pathways were depicted on the y-axis. The x-axis displayed the number of DEPs in each pathway. (**C**) Hierarchical clustering of DEPs in the glucagon signaling pathway. Each column represented a tissue sample, and each line represented a protein that was differentially expressed. The expression levels of DEPs were indicated by a color scale ranging from blue (low) to red (high). The colors red and blue represent up-and down-regulation, respectively. The case represents female pups with VC deficiency, while the control represents female pups with VC supplementation. (For interpretation of the references to color in this figure legend, the reader is referred to the Web version of this article.)

the specific staining of p-Ser15-PYGL was diffusely distributed in the liver sections, especially around the central vein, and that VC deprivation for 3, 4, or 5 weeks significantly reduced the specific staining of p-Ser15-PYGL in the liver sections of female $Gulo^{-/-}$ pups when compared to VC supplementation for 3, 4, or 5 weeks, respectively (Fig. 3D, H, L). In the female $Gulo^{-/-}$ pups, VC deprivation inactivated glycogen synthase and glycogen phosphorylase under fed and fasting conditions, respectively.

We then used PAS staining and hepatic glycogen measurements to confirm the role of VC deprivation in glycogen storage in female $Gulo^{-/-}$ pups. Female $Gulo^{-/-}$ pups given VC supplement had the same well-organized hepatic cords and levels of PAS staining in their livers as age- and sex-matched wild-type pups, whilst female $Gulo^{-/-}$ pups given the VC deprivation for 3, 4, or 5 weeks had disorganized hepatic cords and lower levels of PAS staining than age- and sex-matched $Gulo^{-/-}$ pups given VC supplement (Fig. 4A–C). Similarly, measurements of hepatic glycogen content revealed that female $Gulo^{-/-}$ pups with VC deprivation for 3, 4, or 5 weeks had significantly lower glycogen content than those with VC supplementation for 3, 4, or 5 weeks (Fig. 4D). Glycogen storage is indeed reduced in female $Gulo^{-/-}$ pups and VC

deprivation is likely to have reduced glycogen storage in the fed condition and, as a result, glycogen output in the fasting condition, eventually leading to hypoglycemia.

3.4. VC deprivation enhanced S-nitrosylation and activation of GSK3β

We measured the activity of GSK3β, which directly phosphorylates GS to inhibit glycogen synthesis [32], to investigate the underlying mechanism by which VC deprivation inactivates GS. Immunohistochemistry staining revealed that p-Ser9-GSK3β was diffusely distributed in liver sections, especially around the central vein, and was more robustly detected in the livers of female $Gulo^{-/-}$ pups with VC supplementation for 3 weeks than with VC deprivation for 3 weeks (Fig. 5A and B). Western blotting analysis confirmed this observation, showing that compared to VC supplementation for 3 weeks, VC deprivation for 3 weeks significantly reduced the levels of p-Ser9-GSK3β (activation of GSK3β) in the livers of female $Gulo^{-/-}$ pups (Fig. 5C and D). Contrarily, western blotting analyses in female $Gulo^{-/-}$ pups with VC deprivation for 3 weeks revealed that VC treatment at 60 μM time-dependently induced the levels of p-Ser9-GSK3β within 30 min of stimulation in
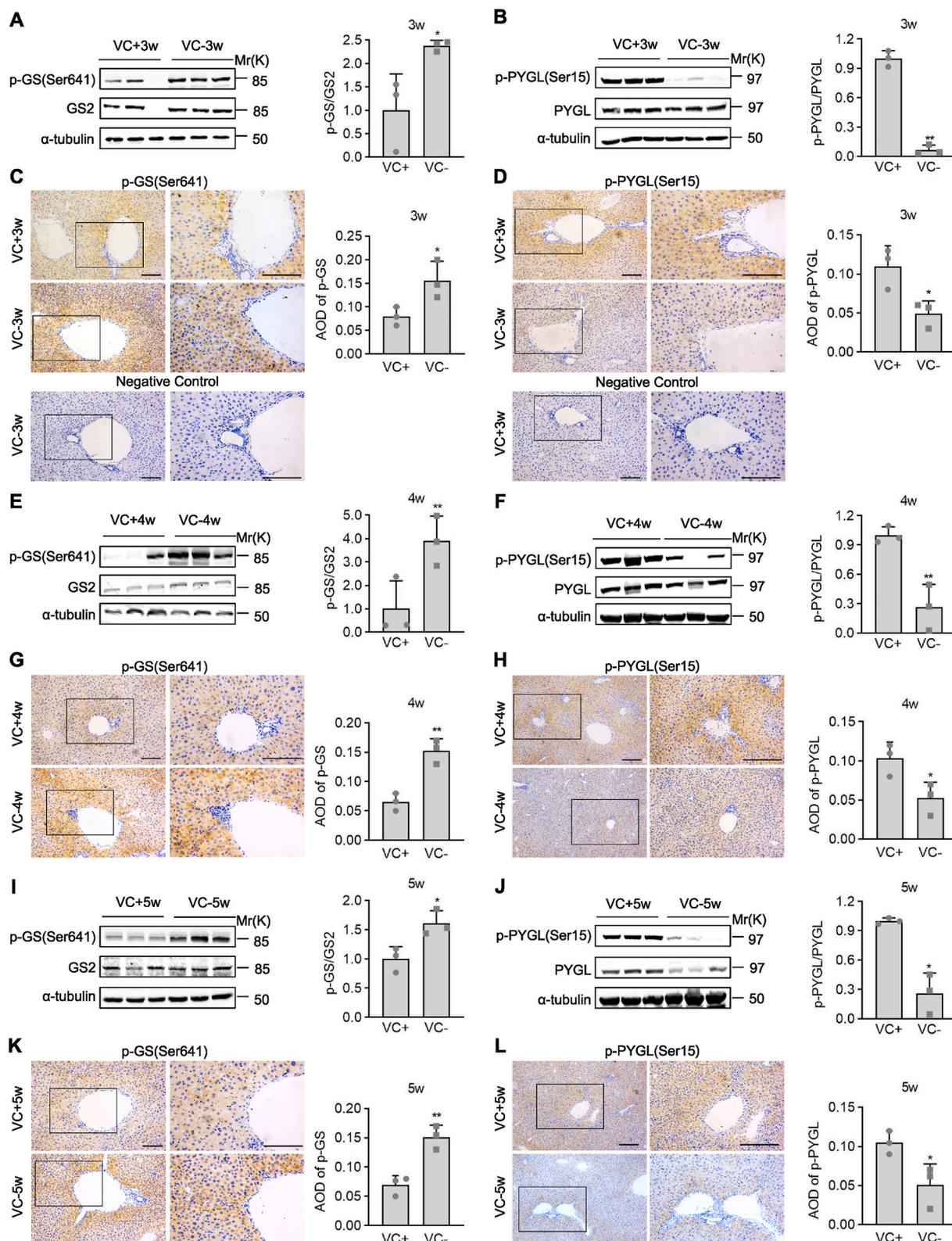
Fig. 3. Female *Gulo*$^{-/-}$ pups' glycogen synthesis and glycogenolysis were affected by VC deprivation. Female *Gulo*$^{-/-}$ pups (six pups per group) were supplemented with 3.3 g/L VC or denied VC in their drinking water for 3, 4, or 5 weeks. Three livers were chosen at random for the following experiments. (**A, B, E, F, I, J**) Western analyses and semi-quantification of p-Ser641-GS, GS2, p-Ser15-PYGL, and PYGL. (**C, D, G, H, K, L**) Immunohistochemistry staining and semi-quantification for p-Ser641-GS and p-Ser15-PYGL. (**C and D**) Negative controls were used to assess the specificity of the immunohistochemistry staining and to rule out false-positive staining reactions. Welch's *t*-test, n = 3, mean SD; *$p < 0.05$, **$p < 0.01$ versus VC+. Square frames define the magnified regions.
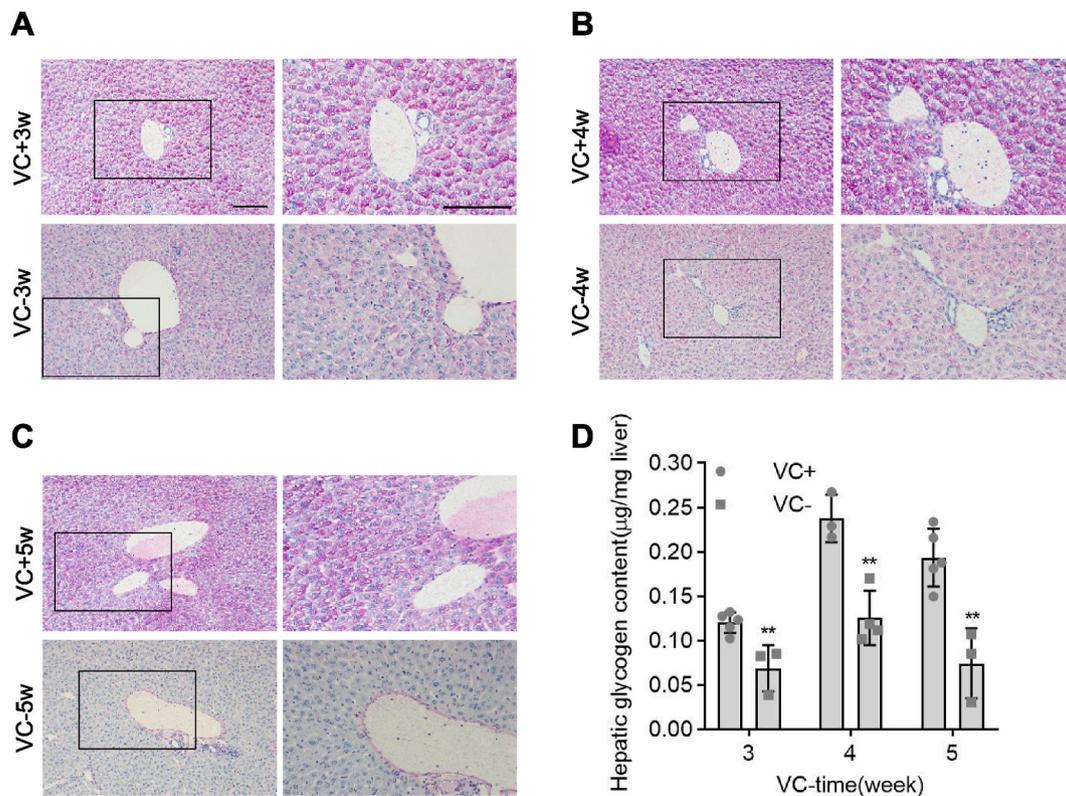
Fig. 4. Glycogen storage was reduced in female *Gulo*$^{-/-}$ pups after VC deprivation. Female *Gulo*$^{-/-}$ pups (5 pups per group) were supplemented with 3.3 g/L VC or devoid of VC in the drinking water for 3, 4, or 5 weeks at 22 days old. The following experiments required the collection of livers. (**A-C**) PAS staining in paraffin-embedded liver sections and representative images. (**D**) Hepatic glycogen levels as measured by biochemistry. Mean SD, n = 5, one-way ANOVA and Dunnett's multiple comparison tests; *$p < 0.05$, **$p < 0.01$ versus VC+. Square frames define the magnified regions.

primary mouse hepatocytes (PMH) (Fig. 5E and F). Also, in human hepatocyte cell line L02 cells, VC treatment consistently increased the levels of p-Ser9-GSK3β in a dose- or time-dependent manner. (Figs. S6A–D). S-nitrosylation, which is defined as the covalent addition of a NO group to a cysteine (Cys) thiol to form S-nitrosothiols (SNOs), is important for protein activity and stability [33,34]. The level of S-nitrosylation of GSK3β was examined after VC deprivation. S-nitrosylated GSK3β levels were significantly increased in the livers of female *Gulo*$^{-/-}$ pups after 3 weeks of VC deprivation, as measured by an iodoTMT labeling strategy (Fig. 5G and H). We used N6022, a specific inhibitor of S-nitrosoglutathione reductase (GSNOR) that induces the denitrosylation of target proteins, to confirm that S-nitrosylation affected GSK3β activity. We found that N6022 significantly reduced p-Ser9-GSK3β levels in a dose- or time-dependent manner in L02 cells (Fig. 5K-N). Similarly, N6022 significantly increased the levels of S-nitrosylated Flag-GSK3β, while VC completely reversed the effect of N6022 in HepG2 cells, transiently expressing Flag-tagged GSK3β (Fig. 5I and J). A NO synthase inhibitor, Nω-Nitro-L-arginine methyl ester (L-NAME), confirmed the link between S-nitrosylation and phosphorylation of GSK3β [35]. L-NAME suppresses NO biosynthesis, reducing the formation of S-nitrosothiols [36,37]. In L02 cells, L-NAME treatment significantly increased p-Ser9-GSK3β levels in a time and dose-dependent manner, as expected (Fig. 5O–R). As a result, VC deprivation activated GSK3β by lowering its S-denitrosylation.

3.5. VC induced the denitrosylation and subsequent inactivation of GSK3β

We investigated the potential relationship between S-nitrosylation and phosphorylation of GSK3β because VC deprivation increased S-nitrosylation and activation of GSK3β. GSK3β's Cys14 was identified as a potential S-nitrosylation residue by bioinformatics (GPS-SNO 1.0), and

sequence alignment revealed a conserved S-nitrosylation Cys14 motif on the GSK3β proteins (Fig. 6A). To determine the potential role of VC in S-nitrosylation of GSK3β at Cys14, we tested the ability of wild-type Flag-tagged GSK3β (WT) and its denitrosylation variant with a mutation at the consensus cysteine residue (Cys14Ser, C14S mutant) to activate GSK3β in response to VC, L-NAME, or N6022 stimulation in HepG2 cells. Flag-p-Ser9-GSK3β levels were significantly higher in HepG2 cells expressing the C14S mutant than in cells expressing the WT, suggesting that GSK3β inactivation was caused by denitrosylation at Cys14 (Fig. 6B–I). Also, VC at 60 μM and L-NAME at 3.2 mM significantly increased Flag-p-Ser9-GSK3β levels in HepG2 cells expressing WT but did not affect Flag-p-Ser9-GSK3β levels in HepG2 cells expressing C14S mutant (Fig. 6B–E). Similarly, at 5 nM, N6022 significantly decreased Flag-p-Ser9-GSK3β levels in HepG2 cells expressing WT but did not affect Flag-p-Ser9-GSK3β levels in HepG2 cells expressing C14S mutant (Fig. 6F and G). Analyzes of the Flag–SNO–GSK3β and Flag-p-Ser9-GSK3β levels after treatment with N6022 revealed that N6022 significantly increased and decreased the Flag–SNO–GSK3β and Flag-p-Ser9-GSK3β levels, respectively, in HepG2 cells expressing WT, whilst N6022 had no effect on the Flag–SNO–GSK3β or Flag-p-Ser9-GSK3β levels in HepG2 cells expressing C14S mutant (Fig. 6H and I), indicating that S-nitrosylation occurred in the GSK3β Cys14 residue to activate GSK3β. So, VC caused GSK3β denitrosylation at Cys14, which rendered GSK3β inactive.

Molecular dynamics simulations using the Amber14 package were used to determine whether VC deprivation-induced S-nitrosylation on Cys14 affected GSK3β kinase activity. The mechanism was determined using 20-ns molecular dynamics simulations based on S-nitrosylation. The root-mean-square deviation (RMSD) values of the protein backbone based on the starting structure were calculated and plotted along the simulation time to investigate the dynamic stability of the complex and to ensure the rationality of the sampling strategy (Fig. S7). During the
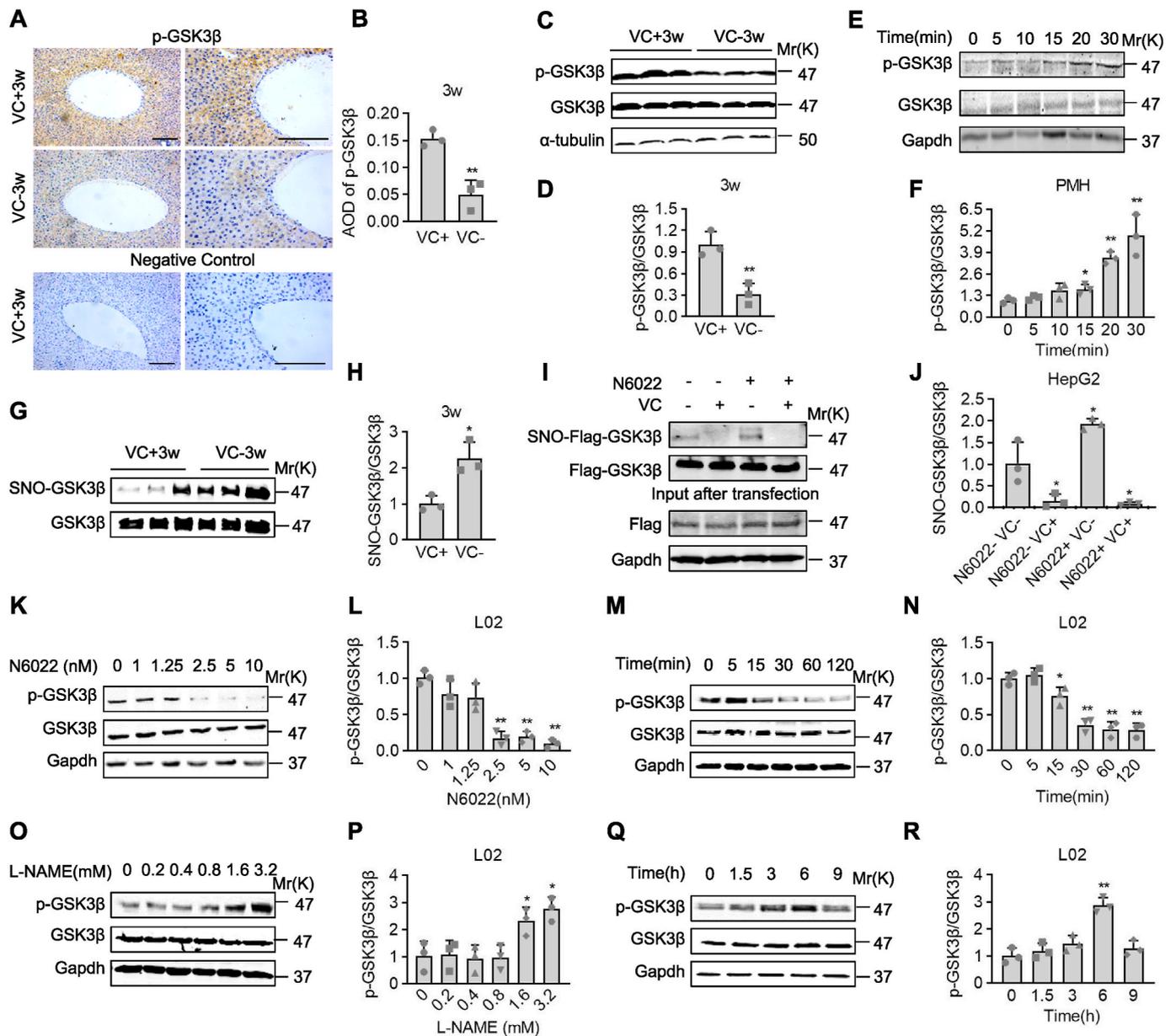
Fig. 5. S-nitrosylation of GSK3β was activated by VC deprivation. (**A-D**) Immunohistochemistry staining, western analyses, and semi-quantification of p-Ser9-GSK3β in the livers of female *Gulo*$^{-/-}$ pups with or without VC supplementation for 3 weeks. (**E and F**) Primary hepatocytes from female *Gulo*$^{-/-}$ pups that had been deprived of VC for 3 weeks were isolated and stimulated with 60 μM VC for the times indicated, followed by western analyses. (**G and H**) An iodoTMT labeling strategy was used to quantify SNO-GSK3β levels in the livers of female *Gulo*$^{-/-}$ pups with or without VC supplementation for 3 weeks. (**I and J**) HepG2 cells were transfected with Flag-GSK3β, then treated with 60 μM VC, 5 nM N6022, or a combination of the two. Protein samples were immunoprecipitated with a Flag antibody before being subjected to iodoTMT labeling and western analyses to detect SNO-GSK3β levels. (**K–N**) Western analyses and semi-quantification in L02 cells after N6022 treatment at the indicated concentrations for 30 min or at 5 nM for the indicated times. (**O-R**) Western analyses and semi-quantification of L02 cells treated with L-NAME at the indicated concentrations for 6 h or at 3.2 mM for the indicated times. Mean SD, n = 3, one-way ANOVA and Dunnett's multiple comparison tests; *$p < 0.05$, **$p < 0.01$ versus lane 1. Square frames define the magnified regions.

20-ns simulation, the system's protein structure was stabilized. The hydroxyl group of Ser9 was exposed to wild-type GSK3β and was very easy to phosphorylate (Fig. 6J, left panel). Ser9 turned inside and formed a hydrogen bond interaction with the residue Lys91 (2.1 Å)) when Cys14 was S-nitrosylated in a 20-ns molecular dynamics simulation, preventing Ser9 from being phosphorylated and retaining GSK3β kinase activity (Fig. 6J, right panel). As a result, the above molecular simulations rationally explained the difference between wild-type and S-nitrosylated GSK3β, as well as the underlying mechanism for GSK3β activation by S-nitrosylation at Cys14.

3.6. L-NAME reversed the VC deprivation-induced hypoglycemia

To learn more about the role of VC deprivation-induced S-nitrosylation in GSK3β activity and glucose homeostasis, we intraperitoneally administrated the female *Gulo*$^{-/-}$ pups with L-NAME at 0.8 mg/10g body weight once a day for 5 weeks. FSG levels showed that giving L-NAME to female *Gulo*$^{-/-}$ pups for 3, 4, and 5 weeks significantly reversed hypoglycemia caused by VC deprivation (Fig. 7A). L-NAME administration in VC-deprived female *Gulo*$^{-/-}$ pups restored the AUC to almost the same level as vehicle administration in VC-supplemented female *Gulo*$^{-/-}$ pups, according to analyzes of FSG values from the end of week 3 to the end of week 5 (Fig. 7B). PAS staining and
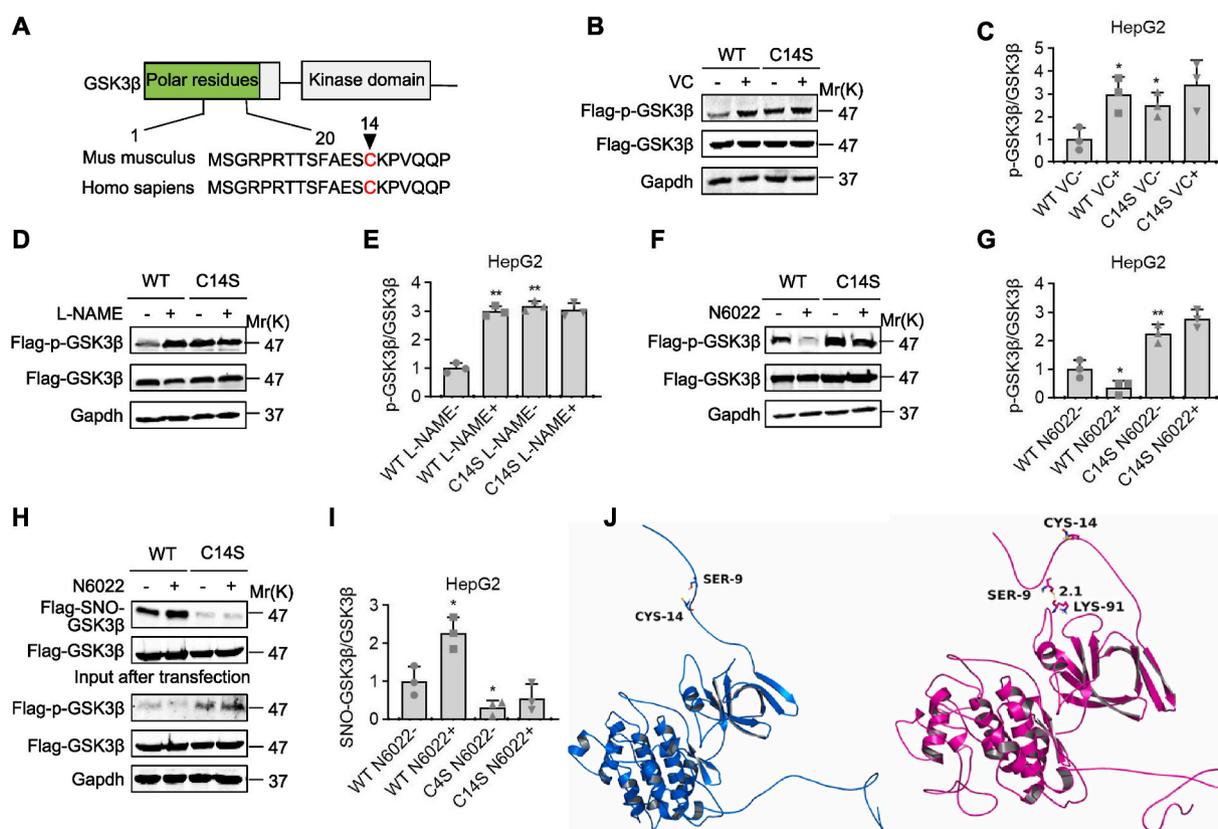
Fig. 6. GSK3β was denitrosylated and inactivated because of VC. (**A**) Protein structure and homology sequence analysis of human and mouse GSK3's first 20 amino acids. (**B-G**) HepG2 cells were transfected with Flag-tagged wild-type GSK3β (WT) or its C14S mutant, then treated for 30 min with 60 µM VC, 6 h with 3.2 mM L-NAME, or 1 h with 5 nM N6022. Protein samples were immunoprecipitated with a Flag antibody before being subjected to western analyses and semi-quantification. (**H and I**) HepG2 cells were transfected with WT or C14S mutant, then treated for 1 h with 5 nM N6022. Protein samples were immunoprecipitated with a Flag antibody and then subjected to iodoTMT labeling to detect SNO-GSK3β levels, western blotting, and semi-quantification. (**J**) GSK3β structural modeling following S-nitrosylation at Cys14. The figures were created using Amber14 and 20-ns molecular dynamics simulations based on S-nitrosylation. Left panel: wild-type GSK3β; right panel: Cys14-S-nitrosylated GSK3β obtained from a 20-ns MD simulation. Mean SD, n = 3, one-way ANOVA and Dunnett's multiple comparison tests; *$p < 0.05$, **$p < 0.01$ versus lane 1.

measurement of glycogen levels in livers showed that L-NAME administration robustly reversed the down-regulation of PAS staining and glycogen levels in the female $Gulo^{-/-}$ pups in response to VC deprivation, and L-NAME administration in the female $Gulo^{-/-}$ pups with VC deprivation caused almost the same levels of PAS staining and glycogen as vehicle administration in the female $Gulo^{-/-}$ pups with VC supplement (Fig. 7C and D). So, L-NAME appeared to reverse hypoglycemia and glycogen synthesis downregulation in female $Gulo^{-/-}$ pups in response to VC deprivation.

We next performed western blotting and immunohistochemistry staining in the livers of female $Gulo^{-/-}$ pups after VC deprivation for 5 weeks to confirm that S-nitrosylation of GSK3β was involved in the reversed effect of L-NAME on the hypoglycemia. L-NAME administration did not affect the female $Gulo^{-/-}$ pups with VC deprivation for 4 weeks' average food and water intake or body weights (Data not shown). SNO-GSK3β levels were measured in the livers, and L-NAME administration significantly reduced the VC deprivation-induced SNO-GSK3β levels (Fig. 7E). Similarly, western blotting and immunostaining analyses revealed that the L-NAME treatment effectively reversed the decrease and increase in p-Ser9-GSK3β and p-Ser641-GS levels in response to VC deprivation, respectively (Fig. 7F–H). Western blotting and immunostaining analyses, on the other hand, revealed that L-NAME did not affect the decrease in p-Ser15-PYGL levels in response to VC deprivation (Fig. S8). So, systemic inhibition of NOS by L-NAME rescued hypoglycemia by counteracting the S-nitrosylation and activation of GSK3β caused by VC deprivation.

3.7. VC deprivation-induced cognitive disorders were rescued by glucose supplement or L-NAME administration

We supplemented the female $Gulo^{-/-}$ pups with VC at 3.3 g/L, glucose at 2 g/L, or neither VC nor glucose for three weeks to determine the pathophysiological significance of VC deprivation-induced hypoglycemia, and assessed long-term memory performance using the Morris water maze. Although glucose supplementation completely corrected hypoglycemia, it did not affect the female $Gulo^{-/-}$ pups' low body weights caused by VC deprivation (Figs. S9A and B). When compared to female $Gulo^{-/-}$ pups with VC supplementation, the female $Gulo^{-/-}$ pups with VC deprivation showed a significant increase in escape latency and a significant decrease in platform crossing, average speed, swimming length, and percent search for trained time (Fig. 8A–E, the first column versus the second column). Supplementation with glucose, on the other hand, partially reversed the VC deprivation-induced increases or decreases in escape latency, platform crossing, average speed, swimming length, and percent search for the trained time in female $Gulo^{-/-}$ pups (Fig. 8A–E, the second column versus the third column). We next deprived the female $Gulo^{-/-}$ pups of VC after weaning and peritoneally administered L-NAME at 0.8 mg/10g body weight once every day for 5 weeks to determine the potential role of S-nitrosylation inhibition by L-NAME in regulating the cognitive disorders caused by VC deprivation. At the end of week 4, the Morris water maze was used to assess cognitive disorders. L-NAME administration in female $Gulo^{-/-}$ pups significantly reversed the increase in escape latency and the decrease in platform crossing in response to VC deprivation, in line with the role of L-NAME in
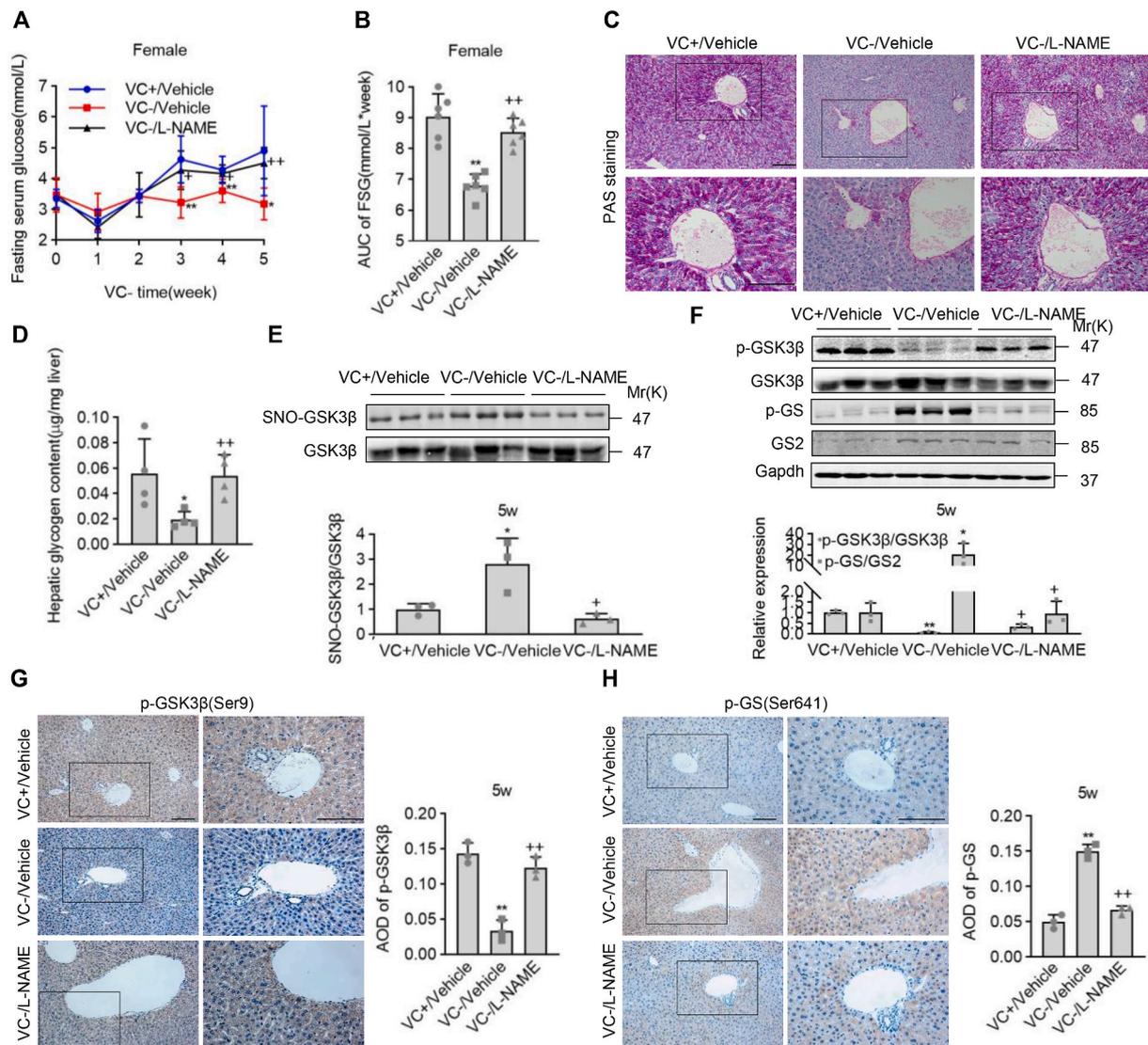
Fig. 7. L-NAME prevented hypoglycemia caused by VC deprivation and S-nitrosylation of GSK3β. Female *Gulo*⁻/⁻ pups were given tap water with or without 3.3 g/L of VC at 22 days old and were injected peritoneally with or without L-NAME at 0.8 mg/10g body weight once daily for five weeks. (**A**) Fasting serum glucose (FSG) levels were measured once a week after a 16-h fast. (**B**) FSG values for the AUC were calculated during a 3 to 5-week period of VC deprivation. (**C-H**) Livers were harvested at the end of week 5 for PAS staining, hepatic glycogen determination, SNO-GSK3β detection by iodoTMT labeling, western blotting, immunohisto-chemistry staining, and semi-quantifications. Mean SD, n = 4, one-way ANOVA and Dunnett's multiple comparison tests; $*p < 0.05$, $**p < 0.01$ versus VC+/Vehicle; $^+p < 0.05$, $^{++}p < 0.01$ versus VC-/Vehicle. Square frames define the magnified regions.

regulating VC deprivation-induced hypoglycemia, though had no effect on the VC deprivation-induced decreases of average speed, swimming length or percent search for the trained time (Fig. 8F–J, the second column versus the third column). In the female *Gulo*⁻/⁻ pups, supplementation with glucose or treatment with L-NAME partially alleviated the cognitive disorders caused by VC deprivation.

4. Discussion

To our knowledge, this is the first study to show that VC deprivation causes hypoglycemia and subsequent cognitive disorders in female pups using a combination of biochemical and genetic approaches. In this molecular event, VC deprivation induces the S-nitrosylation of GSK3β at Cys14, which activates GSK3β and in turn inactivate GS2, to decrease the glycogen synthesis and storage under the fed condition, and meanwhile VC deprivation inactivates GP (PYGL) to inhibit glycogenolysis under the fasting condition, eventually leading to the hypoglycemia and cognitive disorders (Fig. 8K).

L-gulonolactone oxidase handles the oxidation of L-gulonolactone to

L-ascorbic acid (VC), the last step in the pathway, and is deficient in bats, guinea pigs, and humans because of mutations in this gene [38]. *Gulo*⁻/⁻ mice were used to mimic VC metabolism in humans and reveal the specific role of VC deficiency in hypoglycemia. As a result, this study shows the mutual interplay between VC biosynthesis and glucose metabolism, possibly in humans, and expands the list of biological functions influenced by VC. We deprived the 8-week-old female and male *Gulo*⁻/⁻ mice of VC and monitored FSG levels; however, VC deprivation for three weeks had no significant effect on FSG levels in these adult mice (data not shown). VC deprivation-induced hypoglyce-mia was persistent in female pups from 6- to 8-weeks-old, but only in male pups from 8-weeks-old. Because VC deprivation for 5 weeks affected the survival status of mice, even resulting in death, we could not investigate the role of VC deprivation in glucose homeostasis in male *Gulo*⁻/⁻ mice. The pups used in this study were 3–8 weeks old, corresponding to preschool, school, and adolescence in humans based on sexual maturity [39]. Considering these findings, we hypothesized that VC deprivation induces hypoglycemia in an age- and sex-specific manner and that sex hormones may be responsible for the differences
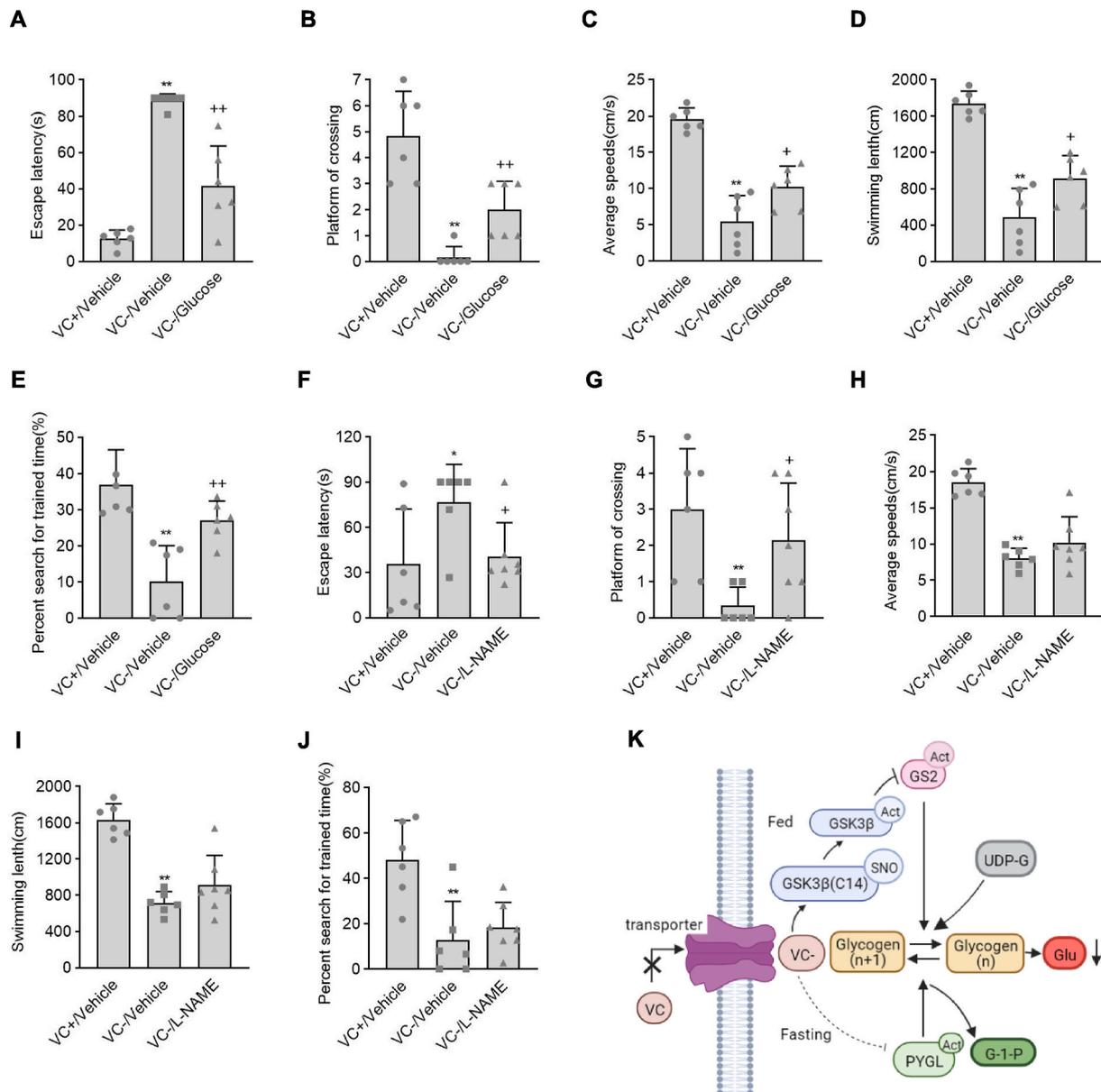
Fig. 8. Hypoglycemia and cognitive disorders caused by VC deprivation were alleviated by glucose supplementation or L-NAME administration. For three weeks, female *Gulo*$^{-/-}$ pups were randomly given tap water containing 3.3 g/L of VC and no glucose (VC+/Vehicle), 2 g/L of glucose and no VC (VC-/Glucose), or neither VC nor glucose (VC-/Vehicle). Alternatively, female *Gulo*$^{-/-}$ pups supplemented with or without VC were injected peritoneally once daily with (+) or without (−) L-NAME at 0.8 mg/10g body weight for 4 weeks. These puppies were then tested for learning and memory abilities using a Morris water maze. (**A and F**) Escape latency, (**B and G**) Platform of crossing, (**C and H**) Average speeds, (**D and I**) Swimming length, (**E and J**) Percent search for trained time. Mean SE, n = 6, one-way ANOVA and Dunnett's multiple comparison tests; *$p < 0.05$, **$p < 0.01$ versus VC+/Vehicle, $^{+}p < 0.05$, $^{++}p < 0.01$ versus VC-/Vehicle. (**K**) A schematic diagram showing the proposed model for VC deprivation-induced hypoglycemia.

between male and female pups [40].

The effects of VC deprivation on hepatic glucose metabolism suggested that VC deprivation affected glycogen synthesis and glycogenolysis, rather than gluconeogenesis or peripheral glucose uptake. The inactivation of PYGL was consistently linked to the exhaustion of glycogen content following inhibited glycogen synthesis or activated glycogenolysis [41]. Though the exact mechanism underlying VC deprivation-inactivating PYGL is unknown, we hypothesize that VC deprivation reduces glycogen storage under the fed condition and glycogen output under the fasting condition, resulting in hypoglycemia. Notably, systemic inhibition of S-nitrosylation by L-NAME almost completely reversed the hypoglycemia caused by VC deprivation, indicating that glycogen synthesis outweighs glycogenolysis in the control of hypoglycemia caused by VC deprivation.

VC is involved in the S-nitrosylation and denitrosylation of target proteins, which is linked to endothelial dysfunction in a variety of cardiovascular diseases [42,43]. Because VC, a powerful antioxidant, uncouples NO from a protein cysteine residue's reactive thiol group and decomposes an S-nitrosothiol [12,13], VC deprivation-induced S-nitrosylation of GSK3β at Cys14 actually results from decreased denitrosylation of GSK3β at Cys14. S-nitrosylation-dependent inhibition of protein-tyrosine phosphatases activity [44], the conversion of nitrosylated aldose reductase to its basal or reduced state by intracellular reductants such as GSH and VC [12], and S-nitrosylation-dependent protein kinase B (AKT) inactivation [45] have all been reported in previous studies. GSK3β is inactivated by AKT [3], and AKT inactivation caused by S-nitrosylation can also activate GSK3β. As a result, VC deprivation is likely to cause S-nitrosylation and inactivation of AKT to

activate GSK3β. To solve this problem, more experiment is required. The link between S-nitrosylation and activation of GSK3β is supported by not only the present but also the previous studies showing that inhibition of NOS by L-NAME inactivated GSK3β in neural stem cells [35], and that L-NAME increased hepatic glycogen content probably by inactivating GSK3β [46].

Previous research has found a strong link between VC deficiency and cognitive disorders. By functional single nucleotide variants (SNVs) of VC transporter genes, altered VC levels in the brain increase the risk of developing cognitive decline associated with Apolipoprotein E E4 (APOE4) [47], and plasma VC levels correlate with markers of the metabolic health and cognitive impairment to a large extent [48]. VC deficiency is common in older hospitalized patients and is associated with cognitive impairment, according to a cross-sectional study [49]. The studies cited above, however, did not explain the mechanism of VC deficiency-induced cognitive disorders. Interestingly, this study found that both glucose supplement and L-NAME administration could partially alleviate the VC deprivation-induced cognitive disorders, which may shed new light on the link between hypoglycemia and cognitive disorders caused by VC deficiency. Different from glucose supplement, L-NAME administration merely significantly reversed the increase in escape latency and the decrease in platform crossing but had no effects on the decreases of average speed, swimming length or percent search for the trained time (indicators of athletic abilities) in response to VC deprivation. Since glucose could provide energy directly after being absorbed into the bloodstream [50,51], we hypothesized that glucose supplement not only partially alleviated the cognitive disorders, but also ameliorated the decline of athletic abilities in VC-deprived female *Gulo*$^{-/-}$ pups. However, L-NAME administration was unable to provide energy directly, thus merely alleviated the cognitive disorders by correcting hypoglycemia in VC-deprived female *Gulo*$^{-/-}$ pups, which may be responsible for the difference.

Summarily, the findings show VC plays a critical role in glucose homeostasis and that VC supplementation in the prevention of hypoglycemia and even cognitive disorders should be considered in certain populations, particularly young female children.

Author contributions

Y.S., Y.C., Q.H., M.Q. Y.C. C.X., and L.T. conducted experiments. Y.S., C.Z., and X.W. analyzed the data and wrote the manuscript. Y.S., C.Z., and X.W. designed experiments. Y.S., C.Z., Q.H., L.T., and X.W. contributed to discussion and reviewed and edited the manuscript. C.Z. and X.W. are the guarantors of this work.

Funding

Declaration of competing interest

No potential conflicts of interest relevant to this article were reported.

Appendix A. Supplementary data

Supplementary data to this article can be found online at https://doi.org/10.1016/j.redox.2022.102420.

References

[1] M.C. Petersen, D.F. Vatner, G.I. Shulman, Regulation of hepatic glucose metabolism in health and disease, Nat. Rev. Endocrinol. 13 (2017) 572–587.

[2] A. Méndez-Lucas, J.A. Duarte, N.E. Sunny, S. Satapati, T. He, X. Fu, J. Bermúdez, S. C. Burgess, J.C. Perales, PEPCK-M expression in mouse liver potentiates, not replaces, PEPCK-C mediated gluconeogenesis, J. Hepatol. 59 (2013) 105–113.

[3] T.Y. Liu, C.X. Shi, R. Gao, H.J. Sun, X.Q. Xiong, L. Ding, Q. Chen, Y.H. Li, J. J. Wang, Y.M. Kang, G.Q. Zhu, Irisin Inhibits Hepatic Gluconeogenesis and Increases Glycogen Synthesis via the PI3K/Akt Pathway in Type 2 Diabetic Mice and Hepatocytes, vol. 129, Clinical science, London, England, 2015, pp. 839–850, 1979.

[4] G. Lefort, M. Haissaguerre, J. Floro, P. Beauffigeau, J.F. Warin, J.L. Latapie, [Hypoglycemia Caused by Overdose of a New Anti-arrhythmia Agent: Cibenzoline. 3 Cases], vol. 17, Presse medicale, Paris, France, 1988, pp. 687–691, 1983.

[5] N. Armaghanian, J.C. Brand-Miller, T.P. Markovic, K.S. Steinbeck, Hypoglycaemia in cystic fibrosis in the absence of diabetes: a systematic review, J. Cyst. Fibros. : Off. J. Eur. Cystic Fibro. Soc. 15 (2016) 274–284.

[6] G. Languren, T. Montiel, A. Julio-Amilpas, L. Massieu, Neuronal damage and cognitive impairment associated with hypoglycemia: an integrated view, Neurochem. Int. 63 (2013) 331–343.

[7] R. Wickström, B. Skiöld, G. Petersson, O. Stephansson, M. Altman, Moderate neonatal hypoglycemia and adverse neurological development at 2-6 years of age, Eur. J. Epidemiol. 33 (2018) 1011–1020.

[8] V. Fernando, X. Zheng, Y. Walia, V. Sharma, J. Letson, S. Furuta, S-nitrosylation: an Emerging Paradigm of Redox Signaling, vol. 8, Antioxidants, Basel, Switzerland, 2019.

[9] S. Duan, C. Chen, S-nitrosylation/denitrosylation and apoptosis of immune cells, Cell. Mol. Immunol. 4 (2007) 353–358.

[10] C.G. Zou, N.S. Agar, G.L. Jones, Enhancement of glutathione-dependent haemin degradation by ascorbic acid, Biochem. Pharmacol. 64 (2002) 565–572.

[11] Y.B. Zhu, Y.P. Zhang, J. Zhang, Y.B. Zhang, Evaluation of vitamin C supplementation on kidney function and vascular reactivity following renal ischemic injury in mice, Kidney Blood Pres. Res. 41 (2016) 460–470.

[12] S.P. Baba, K. Wetzelberger, J.D. Hoetker, A. Bhatnagar, Posttranslational glutathiolation of aldose reductase (AKR1B1): a possible mechanism of protein recovery from S-nitrosylation, Chem. Biol. Interact. 178 (2009) 250–258.

[13] B. Al-Ani, P.W. Hewett, S. Ahmed, M. Cudmore, T. Fujisawa, S. Ahmad, A. Ahmed, The release of nitric oxide from S-nitrosothiols promotes angiogenesis, PLoS One 1 (2006) e25.

[14] X. Ji, X. Hu, C. Zou, H. Ruan, X. Fan, C. Tang, W. Shi, L. Mei, H. Zhu, M. Hussain, L. Zeng, X. Zhang, X. Wu, Vitamin C deficiency exacerbates diabetic glomerular injury through activation of transforming growth factor-β signaling, Biochim. Biophys. Acta Gen. Subj. 1861 (2017) 2186–2195.

[15] Z. Qing, W. Xiao-Hui, W. Xi-Mei, Z. Chao-Chun, Vitamin C deficiency aggravates tumor necrosis factor α-induced insulin resistance, Eur. J. Pharmacol. 829 (2018) 1–11.

[16] D.F. Garcia-Diaz, J. Campion, F.I. Milagro, N. Boque, M.J. Moreno-Aliaga, J. A. Martinez, Vitamin C inhibits leptin secretion and some glucose/lipid metabolic pathways in primary rat adipocytes, J. Mol. Endocrinol. 45 (2010) 33–43.

[17] M. Mattila, I. Erlund, H.S. Lee, S. Niinistö, U. Uusitalo, C. Andrén Aronsson, S. Hummel, H. Parikh, S.S. Rich, W. Hagopian, J. Toppari, Å. Lernmark, A. G. Ziegler, M. Rewers, J.P. Krischer, J.M. Norris, S.M. Virtanen, Plasma ascorbic acid and the risk of islet autoimmunity and type 1 diabetes: the TEDDY study, Diabetologia 63 (2020) 278–286.

[18] A.E. Ratajczak, A. Szymczak-Tomczak, M. Skrzypczak-Zielińska, A.M. Rychter, A. Zawada, A. Dobrowolska, I. Krela-Kaźmierczak, Vitamin C deficiency and the risk of osteoporosis in patients with an inflammatory bowel disease, Nutrients 12 (2020).

[19] M. Weinstein, P. Babyn, S. Zlotkin, An orange a day keeps the doctor away: scurvy in the year 2000, Pediatrics 108 (2001) E55.

[20] N. Hongsawong, N. Chawprang, K. Kittisakmontri, P. Vittayananan, K. Srisuwan, W. Chartapisak, Vitamin C deficiency and impact of vitamin C administration among pediatric patients with advanced chronic kidney disease, Pediatr. Nephrol. 36 (2021) 397–408.

[21] A.C. Carr, S. Rowe, Factors affecting vitamin C status and prevalence of deficiency: a global health perspective, Nutrients 12 (2020).

[22] S. Rowe, A.C. Carr, Global vitamin C status and prevalence of deficiency: a cause for concern? Nutrients 12 (2020).

[23] M.J. Guery, C. Douillard, S. Marcelli-Tourvieille, D. Dobbelaere, J.L. Wemeau, M. C. Vantyghem, Doctor, my son is so tired... about a case of hereditary fructose intolerance, Ann. Endocrinol. 68 (2007) 456–459.

[24] T. Nanjidsuren, C.W. Park, B.W. Sim, S.U. Kim, K.T. Chang, M.H. Kang, K.S. Min, GRK5-Knockout mice generated by TALEN-mediated gene targeting, Anim. Biotechnol. 27 (2016) 223–230.

[25] W.I. Choi, J.H. Yoon, J.Y. Song, B.N. Jeon, J.M. Park, D.I. Koh, Y.H. Ahn, K.S. Kim, I.K. Lee, M.W. Hur, Zbtb7c is a critical gluconeogenic transcription factor that induces glucose-6-phosphatase and phosphoenylpyruvate carboxykinase 1 genes expression during mice fasting, Biochim. Biophys. Acta Gen. Regul. Mech. (2019) 643–656, 1862.

[26] Saqier, S. Bao, S. Han, W. Ao, Effects of Agriophyllum squarrosum extracts on glucose metabolism in KKAy mice and the associated underlying mechanisms, J. Ethnopharmacol. 241 (2019), 112009.

[27] D. Zhang, X. Tong, K. VanDommelen, N. Gupta, K. Stamper, G.F. Brady, Z. Meng, J. Lin, L. Rui, M.B. Omary, L. Yin, Lipogenic transcription factor ChREBP mediates fructose-induced metabolic adaptations to prevent hepatotoxicity, J. Clin. Invest. 127 (2017) 2855–2867.

[28] X. Hu, X. Ji, M. Yang, S. Fan, J. Wang, M. Lu, W. Shi, L. Mei, C. Xu, X. Fan, M. Hussain, J. Du, J. Wu, X. Wu, Cdc42 is essential for both articular cartilage

degeneration and subchondral bone deterioration in experimental osteoarthritis, J. Bone Miner. Res. 33 (2018) 945–958.

[29] H.S. Chung, C.I. Murray, V. Venkatraman, E.L. Crowgey, P.P. Rainer, R.N. Cole, R. D. Bomgarden, J.C. Rogers, W. Balkan, J.M. Hare, D.A. Kass, J.E. Van Eyk, Dual labeling biotin switch assay to reduce bias derived from different cysteine subpopulations: a method to maximize S-nitrosylation detection, Circ. Res. 117 (2015) 846–857.

[30] L.L. Chen, M.L. Wu, F. Zhu, J.J. Kai, J.Y. Dong, X.M. Wu, L.H. Zeng, Neural progenitor cells rptor ablation impairs development but benefits to seizure-induced behavioral abnormalities, CNS Neurosci. Ther. 22 (2016) 1000–1008.

[31] L. Agius, Role of glycogen phosphorylase in liver glycogen metabolism, Mol. Aspect. Med. 46 (2015) 34–45.

[32] J. Lee, M.S. Kim, The role of GSK3 in glucose homeostasis and the development of insulin resistance, Diabetes Res. Clin. Pract. 77 (Suppl 1) (2007) S49–S57.

[33] J. Li, Y. Zhang, Y. Zhang, S. Lü, Y. Miao, J. Yang, S. Huang, X. Ma, L. Han, J. Deng, F. Fan, B. Liu, Y. Huo, Q. Xu, C. Chen, X. Wang, J. Feng, GSNOR modulates hyperhomocysteinemia-induced T cell activation and atherosclerosis by switching Akt S-nitrosylation to phosphorylation, Redox Biol. 17 (2018) 386–399.

[34] L. Jin, Y. Cao, T. Zhang, P. Wang, D. Ji, X. Liu, H. Shi, L. Hua, R. Yu, S. Gao, Effects of ERK1/2 S-nitrosylation on ERK1/2 phosphorylation and cell survival in glioma cells, Int. J. Mol. Med. 41 (2018) 1339–1348.

[35] S.J. Kim, M.S. Lim, S.K. Kang, Y.S. Lee, K.S. Kang, Impaired functions of neural stem cells by abnormal nitric oxide-mediated signaling in an in vitro model of Niemann-Pick type C disease, Cell Res. 18 (2008) 686–694.

[36] G. Tong, A.M. Aponte, M.J. Kohr, C. Steenbergen, E. Murphy, J. Sun, Postconditioning leads to an increase in protein S-nitrosylation, Am. J. Physiol. Heart Circ. Physiol. 306 (2014) H825–H832.

[37] E. Zuccolo, U. Laforenza, S. Negri, L. Botta, R. Berra-Romani, P. Faris, G. Scarpellino, G. Forcaia, G. Pellavio, G. Sancini, F. Moccia, Muscarinic M5 receptors trigger acetylcholine-induced Ca(2+) signals and nitric oxide release in human brain microvascular endothelial cells, J. Cell. Physiol. 234 (2019) 4540–4562.

[38] J.J. Burns, C. Evans, The synthesis of L-ascorbic acid in the rat from D-glucuronolactone and L-gulonolactone, J. Biol. Chem. 223 (1956) 897–905.

[39] S. Dutta, P. Sengupta, Men and mice: relating their ages, Life Sci. 152 (2016) 244–248.

[40] G. Corona, V.A. Giagulli, E. Maseroli, L. Vignozzi, A. Aversa, M. Zitzmann, F. Saad, E. Mannucci, M. Maggi, Therapy of endocrine disease: testosterone supplementation and body composition: results from a meta-analysis study, Eur. J. Endocrinol. 174 (2016) R99–R116.

[41] J.J. Winnick, G. Kraft, J.M. Gregory, D.S. Edgerton, P. Williams, I.A. Hajizadeh, M. Z. Kamal, M. Smith, B. Farmer, M. Scott, D. Neal, E.P. Donahue, E. Allen, A. D. Cherrington, Hepatic glycogen can regulate hypoglycemic counterregulation via a liver-brain axis, J. Clin. Invest. 126 (2016) 2236–2248.

[42] M.B. Morelli, J. Gambardella, V. Castellanos, V. Trimarco, G. Santulli, Vitamin C and Cardiovascular Disease: an Update, vol. 9, Antioxidants, Basel, Switzerland, 2020.

[43] S. Zhao, X. Tang, Z. Miao, Y. Chen, J. Cao, T. Song, D. You, Y. Zhong, Z. Lin, D. Wang, Z. Shi, X. Tang, D. Wang, S. Chen, L. Wang, A. Gu, F. Chen, L. Xie, Z. Huang, H. Wang, Y. Ji, Hsp90 S-nitrosylation at Cys521, as a conformational switch, modulates cycling of Hsp90-AHA1-CDC37 chaperone machine to aggravate atherosclerosis, Redox Biol. 52 (2022), 102290.

[44] D.M. Barrett, S.M. Black, H. Todor, R.K. Schmidt-Ullrich, K.S. Dawson, R. B. Mikkelsen, Inhibition of protein-tyrosine phosphatases by mild oxidative stresses is dependent on S-nitrosylation, J. Biol. Chem. 280 (2005) 14453–14461.

[45] B.L. Slomiany, A. Slomiany, Ghrelin suppression of Helicobacter pylori-induced S-nitrosylation-dependent Akt inactivation exerts modulatory influence on gastric mucin synthesis, Inflammopharmacology 19 (2011) 89–97.

[46] C.A. Tarsitano, V.A. Paffaro Jr., J.R. Pauli, G.H. da Silva, M.J. Saad, I. Salgado, M. A. da Cruz-Höfling, S. Hyslop, Hepatic morphological alterations, glycogen content and cytochrome P450 activities in rats treated chronically with N(omega)-nitro-L-arginine methyl ester (L-NAME), Cell Tissue Res. 329 (2007) 45–58.

[47] K. Hayashi, M. Noguchi-Shinohara, T. Sato, K. Hosomichi, T. Kannon, C. Abe, C. Domoto, S. Yuki-Nozaki, A. Mori, M. Horimoto, M. Yokogawa, K. Sakai, K. Iwasa, K. Komai, M. Ishimiya, H. Nakamura, N. Ishida, Y. Suga, J. Ishizaki, A. Ishigami, A. Tajima, M. Yamada, Effects of functional variants of vitamin C transporter genes on apolipoprotein E E4-associated risk of cognitive decline: the Nakajima study, PLoS One 16 (2021), e0259663.

[48] J.F. Pearson, J.M. Pullar, R. Wilson, J.K. Spittlehouse, M.C.M. Vissers, P.M. L. Skidmore, J. Willis, V.A. Cameron, A.C. Carr, Vitamin C status correlates with markers of metabolic and cognitive health in 50-year-olds: findings of the CHALICE cohort study, Nutrients 9 (2017).

[49] Y. Sharma, A. Popescu, C. Horwood, P. Hakendorf, C. Thompson, Relationship between Vitamin C Deficiency and Cognitive Impairment in Older Hospitalised Patients: A Cross-Sectional Study, Antioxidants, Basel, Switzerland, 2022, p. 11.

[50] Y.K. Li, C.L. Hui, E.H. Lee, W.C. Chang, S.K. Chan, C.M. Leung, E.Y. Chen, Coupling physical exercise with dietary glucose supplement for treating cognitive impairment in schizophrenia: a theoretical model and future directions, Early Interv. Psychiatr. 8 (2014) 209–220.

[51] Q. Zhu, L. Wang, Q. Dong, S. Chang, K. Wen, S. Jia, Z. Chu, H. Wang, P. Gao, H. Zhao, S. Han, Y. Wang, FRET-based glucose imaging identifies glucose signalling in response to biotic and abiotic stresses in rice roots, J. Plant Physiol. 215 (2017) 65–72.